Supplement of Atmos. Chem. Phys. Discuss., 15, 35117–35155, 2015
http://www.atmos-chem-phys-discuss.net/15/35117/2015/
doi:10.5194/acpd-15-35117-2015-supplement

Atmospheric Chemistry and Physics Discussions

Supplement of

Aerosol source apportionment from 1 year measurements at the CESAR tower at Cabauw, NL

P. Schlag et al.

Correspondence to: P. Schlag (p.schlag@fz-juelich.de)

Determination of the Collection Efficiency (CE) algorithm according to Mensah et al. (2012):

1. $CE = 0.5$ for $MF_{NO3} < 0.3$
2. $CE = 1.0$ for $MF_{NO3} = 0.78$
3. $CE = 0.1875 + 1.0417 \times MF_{NO3}$ for $0.3 < MF_{NO3} < 0.78$,

with MF_{NO3} = Mass fraction of ammonium nitrate to total PM_1 mass as measured by the ACSM.

Table S1: Overview of the ambient temperatures and relative humidities during the ACSM campaign, measured at 2 m height.

	Period	Minimum	Maximum	Average
Temperature [°C]	1 (11.07.-30.09.2012)	6.7	32.2	16.5
	2 (01.10.-29.12.2012)	-6.1	21.3	7.7
	3 (08.01.-15.02.2013)	-12.3	12.4	0.6
	4 (18.02.-25.04.2013)	-5.1	19.5	3.5
	5 (25.04.-03.06.2013)	2.9	22.3	10.9
	Entire campaign			9.2
Relative Humidity [%]	1 (11.07.-30.09.2012)	35.7	100.6	79.3
	2 (01.10.-29.12.2012)	51.3	102.6	88.6
	3 (08.01.-15.02.2013)	58.9	102.9	86.2
	4 (18.02.-25.04.2013)	23.2	101.2	72.5
	5 (25.04.-03.06.2013)	35.9	100.3	80.2
	Entire campaign			82.2

Table S2: Fractional abundances of individual aerosol species in % and the average total mass concentrations (Avg) in µg m^{-3}, separated in the five periods and for the entire campaign.

Period	BC	Org	NO_3	SO_4	NH_4	Chl	Avg
1 (11.07.-30.09.2012)	6	35	34	11	13	1	6.1
2 (01.10.-29.12.2012)	8	32	36	13	14	3	7.4
3 (08.01.-15.02.2013)	3	27	43	11	14	1	15.9
4 (18.02.-25.04.2013)	-	27	46	11	16	2	13.2
5 (25.04.-03.06.2013)	5	26	40	12	16	2	10.1
Entire campaign	5	29	39	11	14	2	9.5

Table S3: Fractional abundances of ACSM PMF factors observed for each season and for the entire campaign in % and the respective average organic mass concentrations (Org-Avg) in µg m^{-3}. For the constrained profiles HOA and BBOA, the applied a-value is written in brackets.

Period	HOA	BBOA	OOA	HULIS	Org-Avg
Summer 2012 (11.07.-30.09.2012)	16 (a=0.1)	-	37	47	2.1
Autumn 2012 (01.10.-29.12.2012)	14 (a=0.1)	23 (a=0.2)	21	43	2.4
Winter 2013 (08.01.-27.03.2013)	10 (a=0.1)	15 (a=0.3)	48	27	4.1
Spring 2013 (05.04.-03.06.2013)	8 (a=0.1)	9 (a=0.3)	47	36	2.7
Entire campaign	12	13	38	37	2.8

Table S4: Correlation coefficients (Pearson-R^2) of the comparison between ACSM PMF factor and tracer time series over the entire campaign

Tracer	HOA	BBOA	OOA	HULIS
NO_3	0.28	0.24	0.63	0.39
SO_4	0.14	0.23	0.48	0.41
$NO_3 + SO_4$	0.27	0.26	0.67	0.41
NH_4	0.25	0.23	0.63	0.44
Chl	0.14	0.13	0.04	0.10
BC	0.38	0.39	0.34	0.47
m/z 60 (ACSM)	0.42	0.94	0.39	0.26
Rn (gas phase, 20 m height)	0.30	0.21	0.23	0.34
CO_2 (gas phase, 20 m height)	0.24	0.31	0.24	0.21
NO_x (gas phase)	0.47	0.36	0.07	0.10
CO (gas phase)	0.47	0.49	0.37	0.30

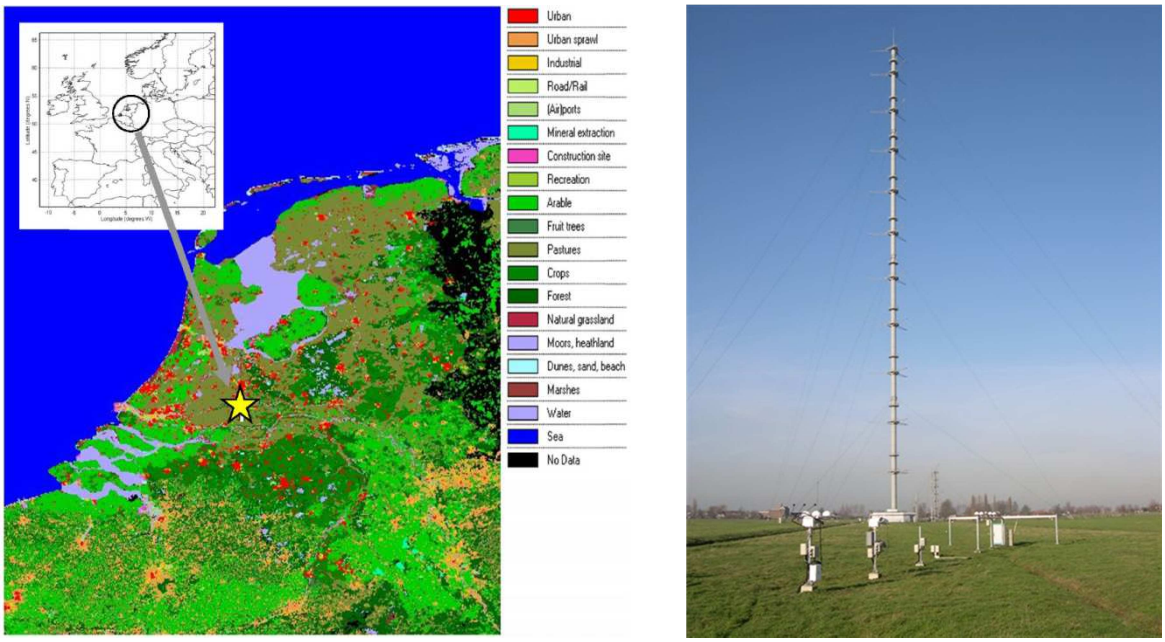

Figure S1: Left: Measurement location; colours define different land use; taken from Vermeulen et al. (2011); Right: Picture of CESAR tower

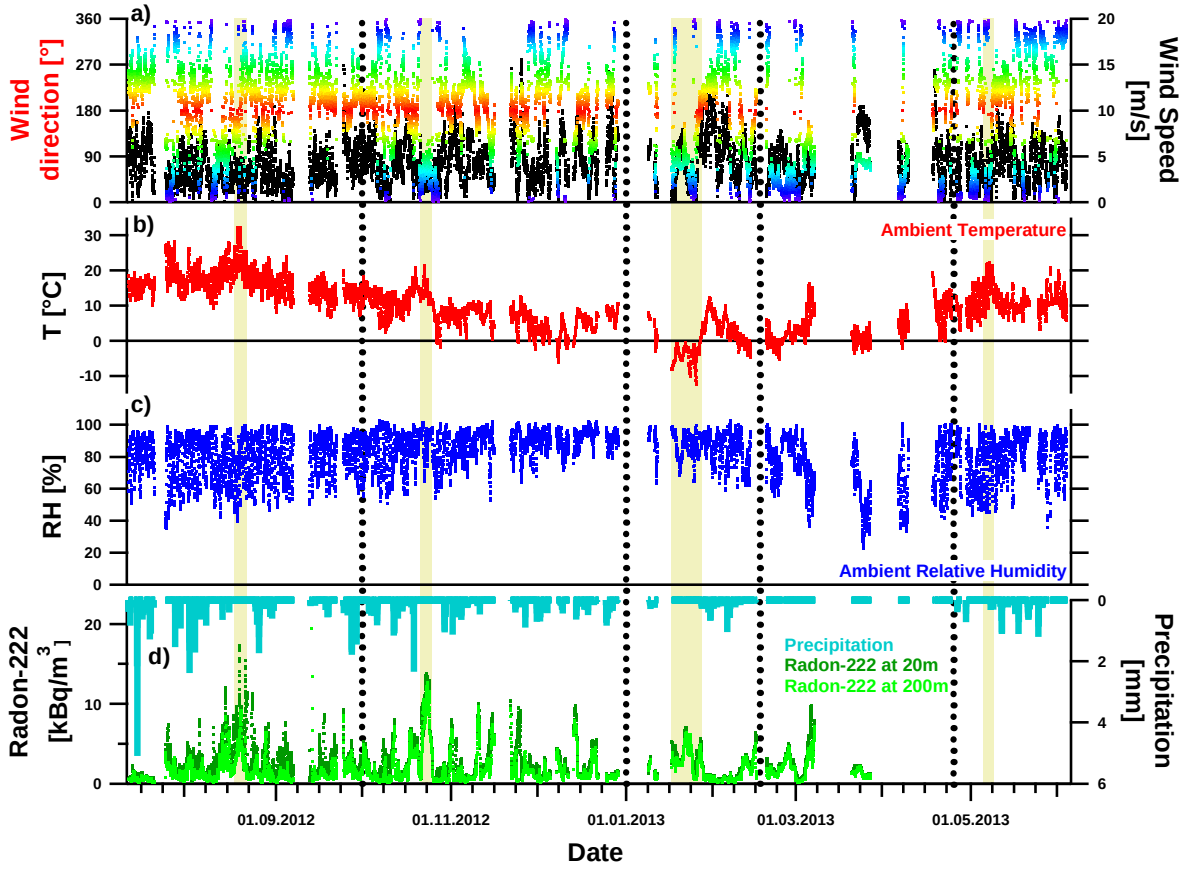

Figure S2: Meteorological overview of the ACSM campaign: a) Wind direction (0°/360°, 90°, 180°, and 270° represent North, East, South, and West, respectively; for a better clearance, the graph is additionally color-coded by degrees) and wind speed (black) at 10 m height. b) and c) temperature and relative humidity at 2 m height. d) Precipitation (turquoise) and Radon-222, measured at 20 m (dark green) and 200 m (light green). Pollution events are indicated by green shaded areas.

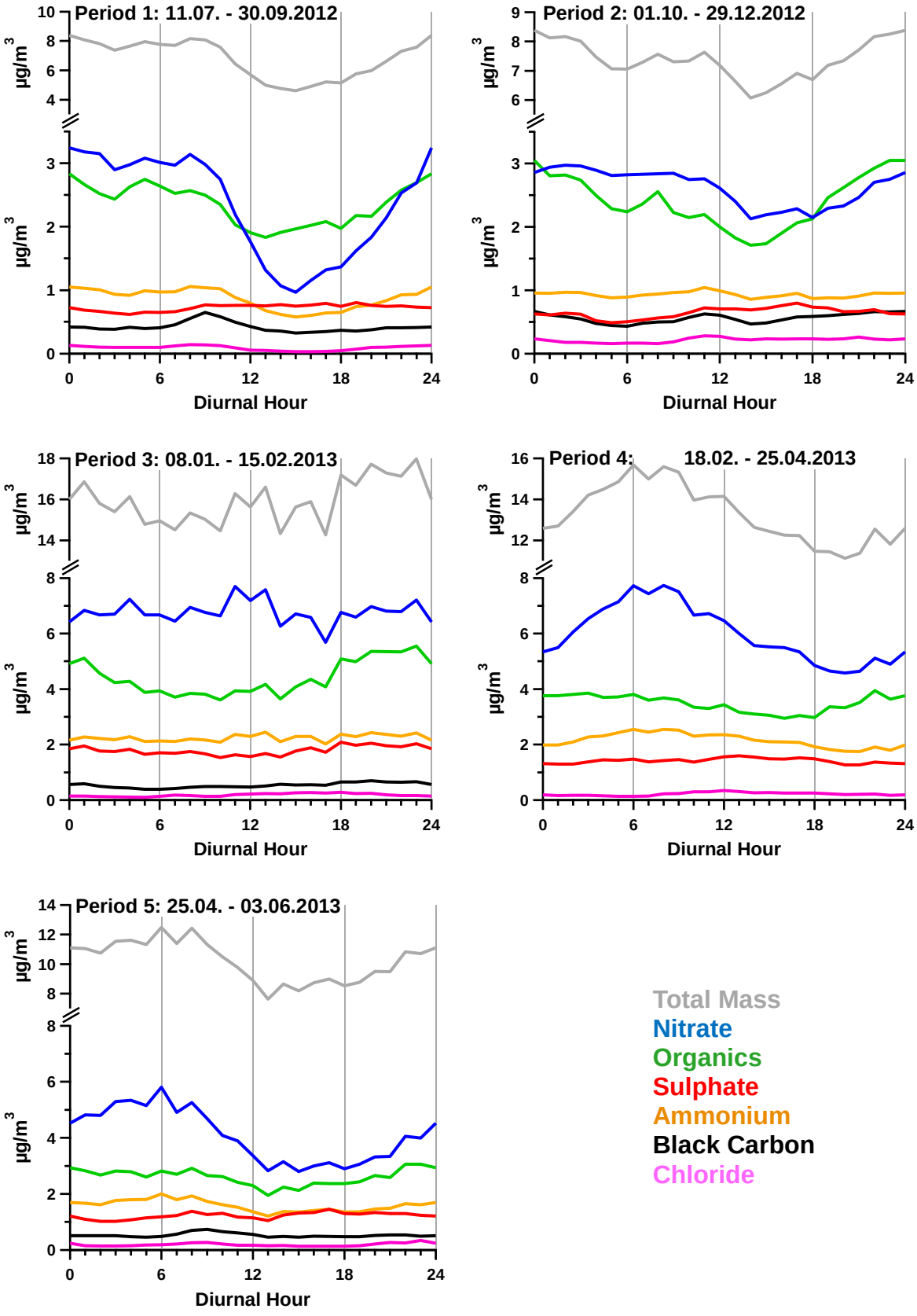

Figure S3: Diurnal variation (local time) of individual species and the total mass, averaged over the entire ACSM campaign and over the five periods, which are explained in Table S1. Note the different scales of y-axes between the periods.

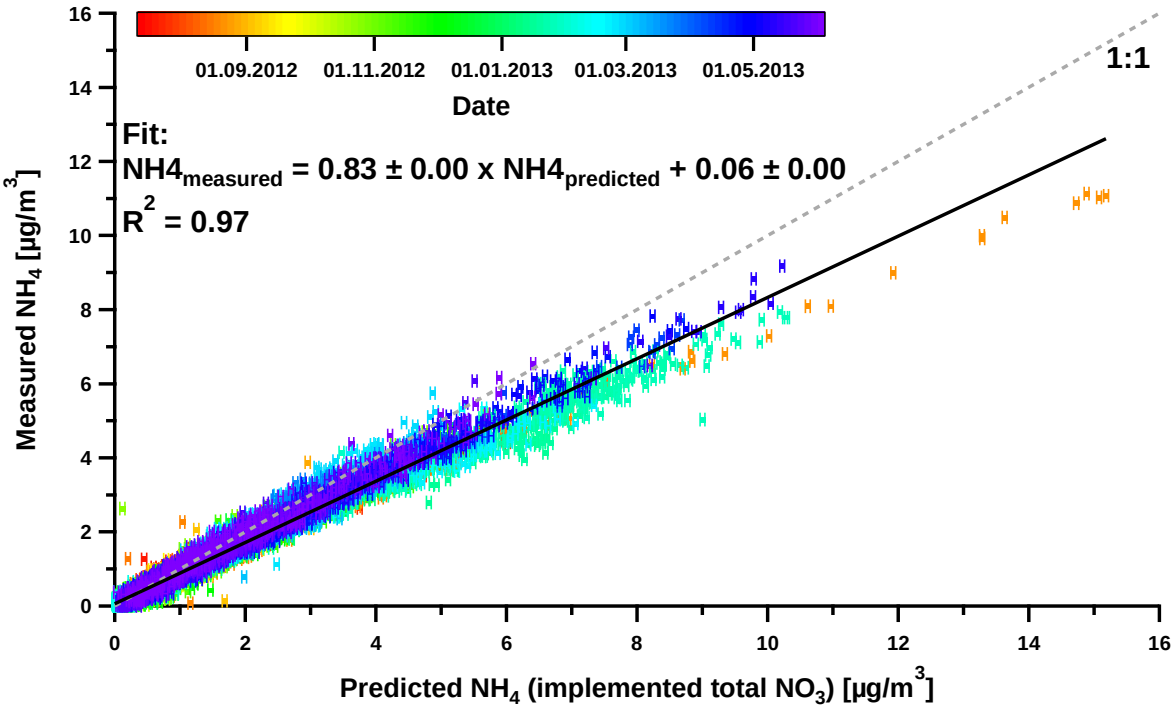

Figure S4: Correlation plot of measured against predicted NH_4 during the ACSM campaign. Error bars represent uncertainties of the NH_4 prediction.

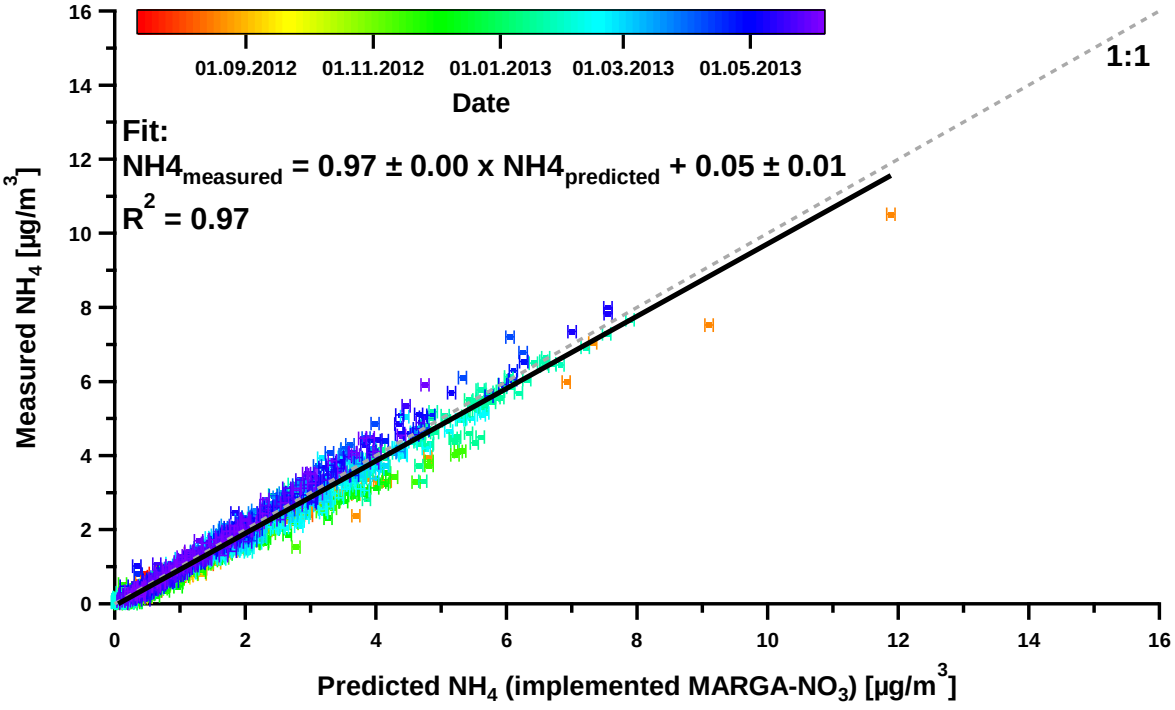

Figure S5: Correlation plot of measured against predicted NH_4 during the ACSM campaign. Here, the MARGA-NO_3 instead of the ACSM-NO_3 was used for the ion balance. Therefore, all time series were averaged to MARGA time prior to the correlation. Error bars represent uncertainties of the NH_4 prediction.

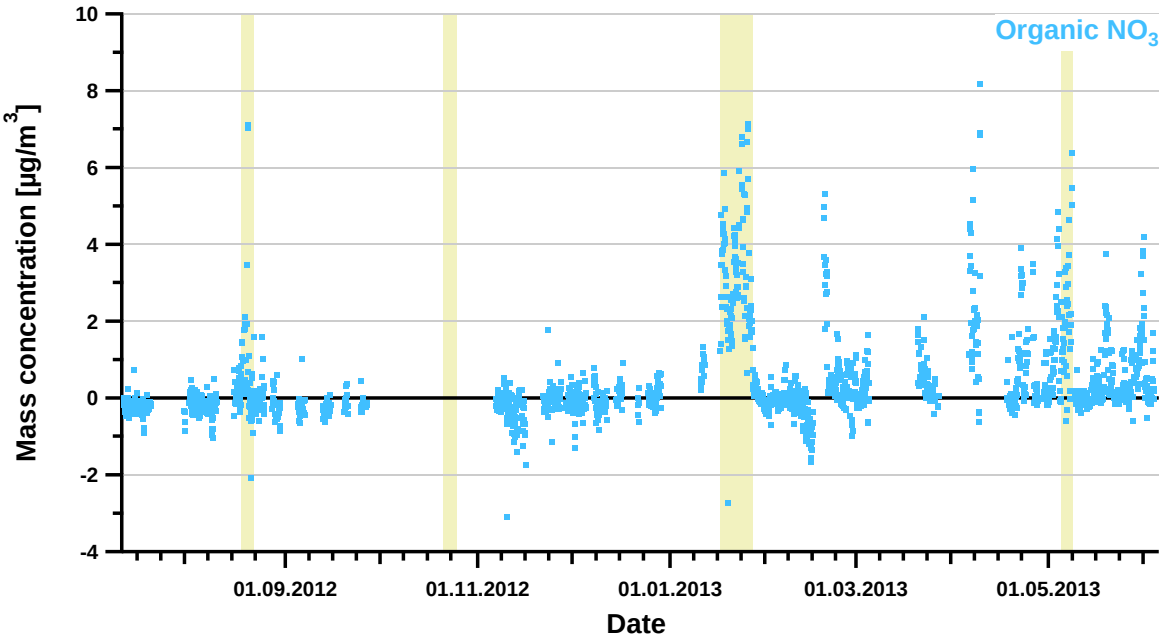

Figure S6: Time series of the ACSM organic nitrate mass concentrations, calculated by subtracting the MARGA-NO_3 from the ACSM-NO_3, according to Sec. 3.1 in the main text. Pollution events are indicated by green shaded areas.

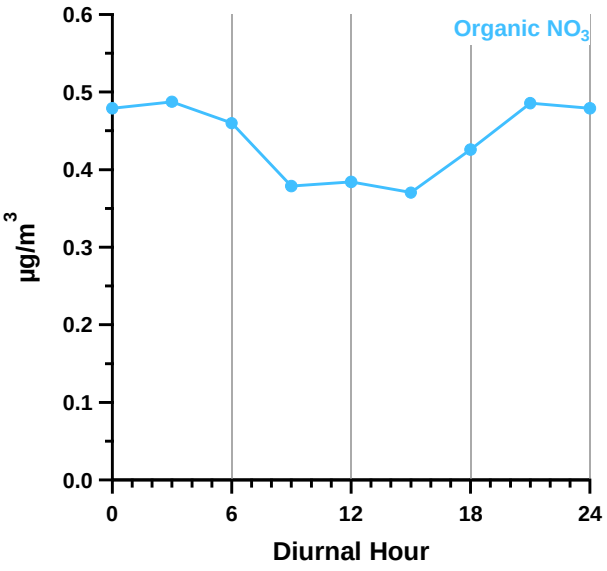

Figure S7: Average diurnal variations (LT) of the AMS organic nitrate concentrations, calculated according to Sec. 3.1 in the main text.

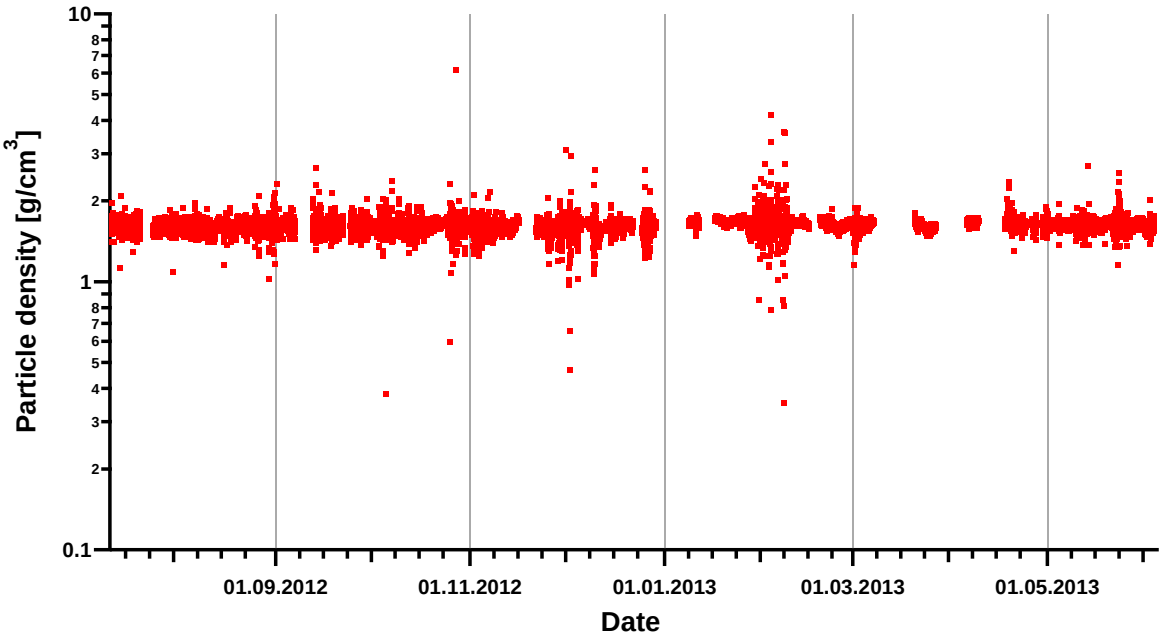

Figure S8: Particle density, determined from ACSM+MAAP aerosol composition as described in Sec. 3.2 in the main text.

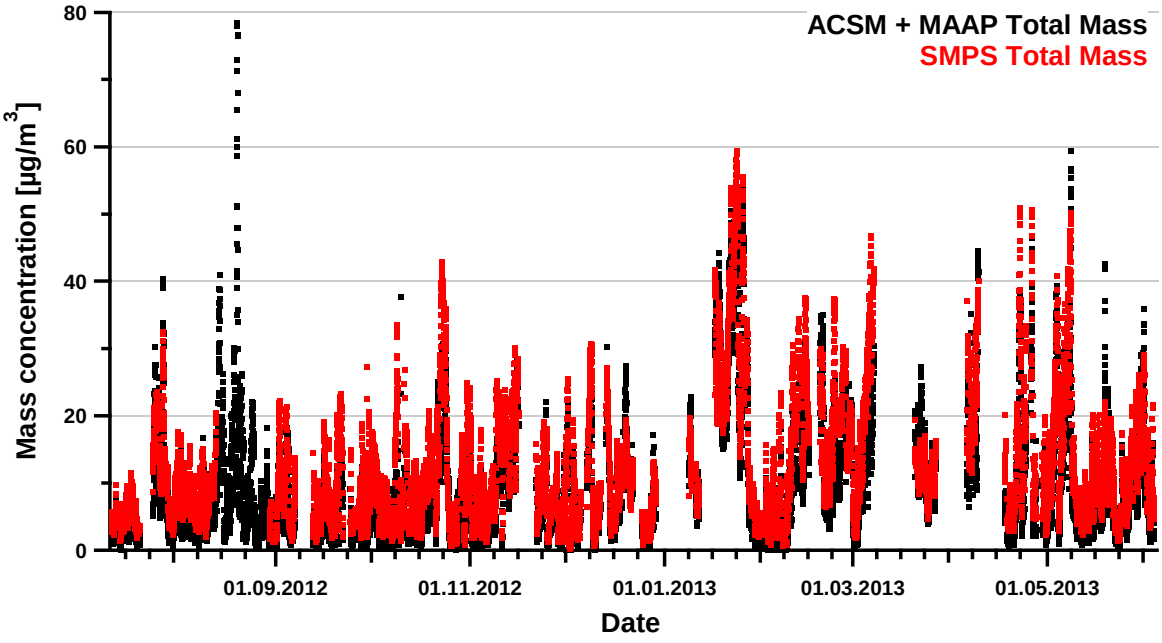

Figure S9: Time series of ACSM+MAAP and SMPS mass concentrations

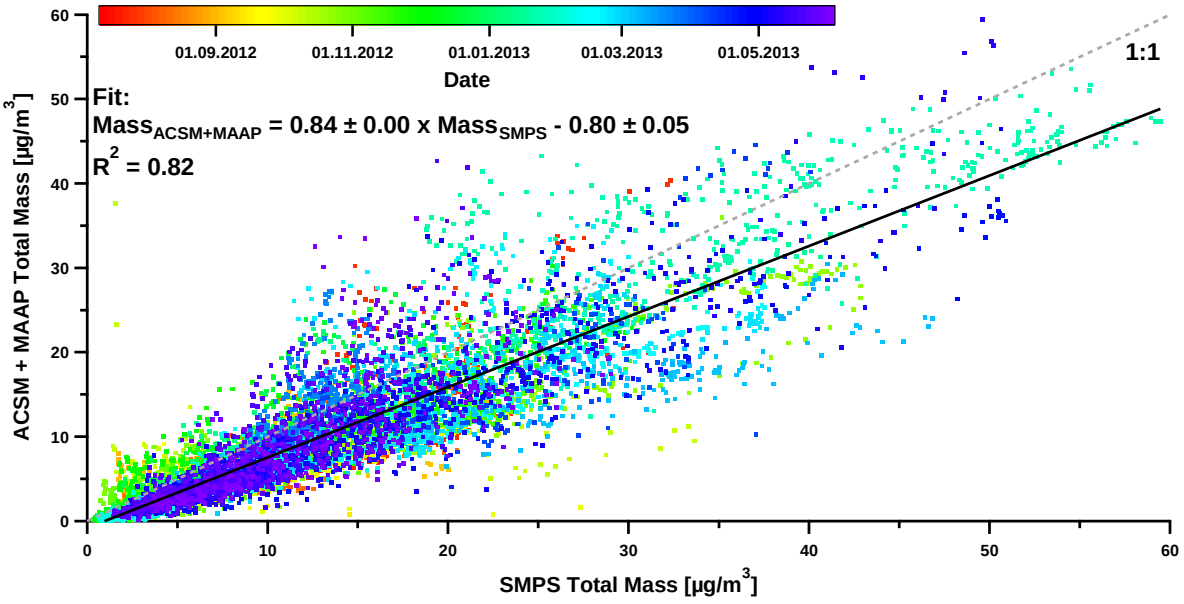

Figure S10: Correlation plot of ACSM+MAAP and SMPS mass concentrations

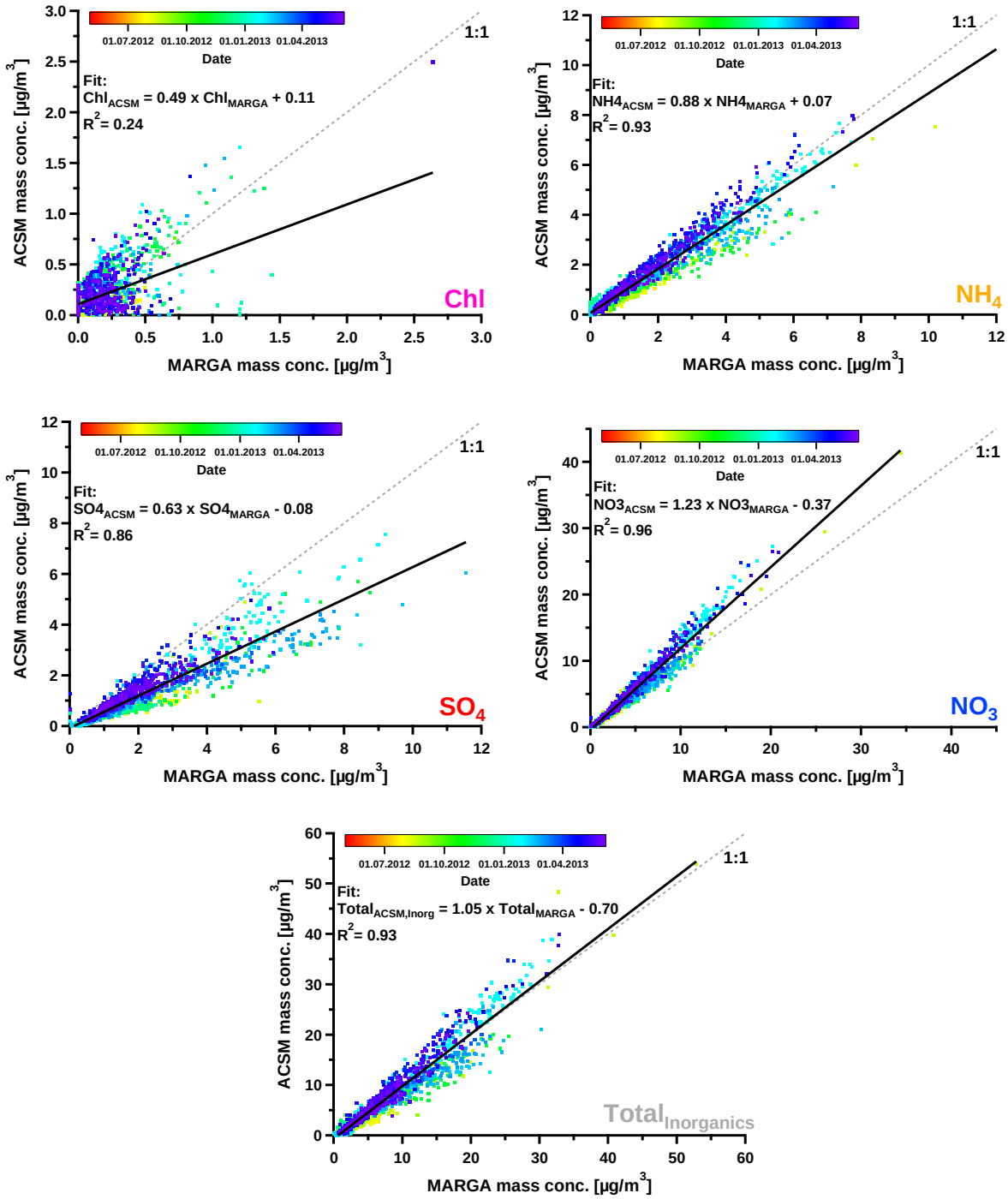

Figure S11: Correlation graphs of Chl, NH_4, SO_4, NO_3, and total inorganic mass concentrations from ACSM and MARGA data

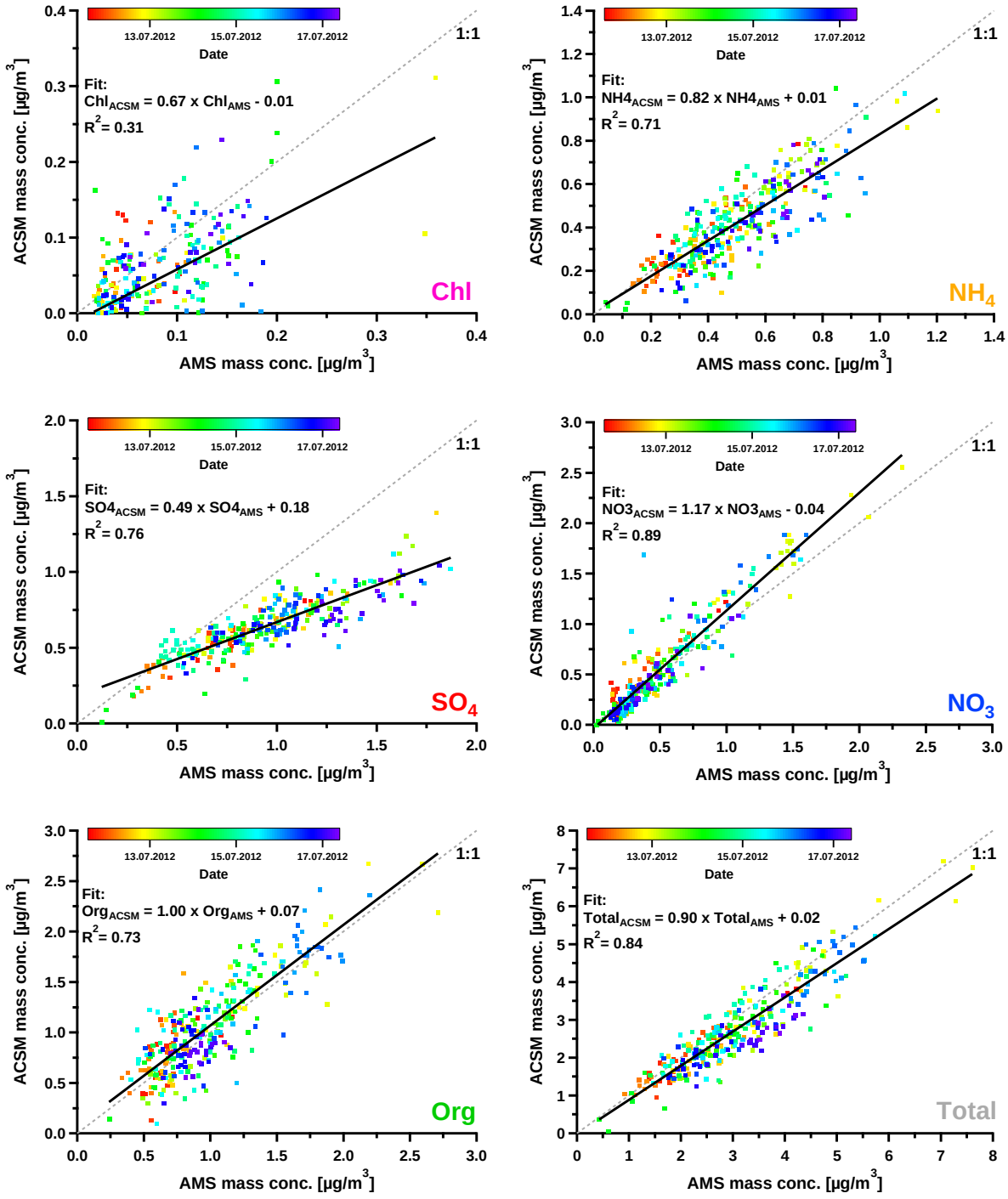

Figure S12: Correlation graphs of individual species and total mass concentrations from ACSM data with AMS data

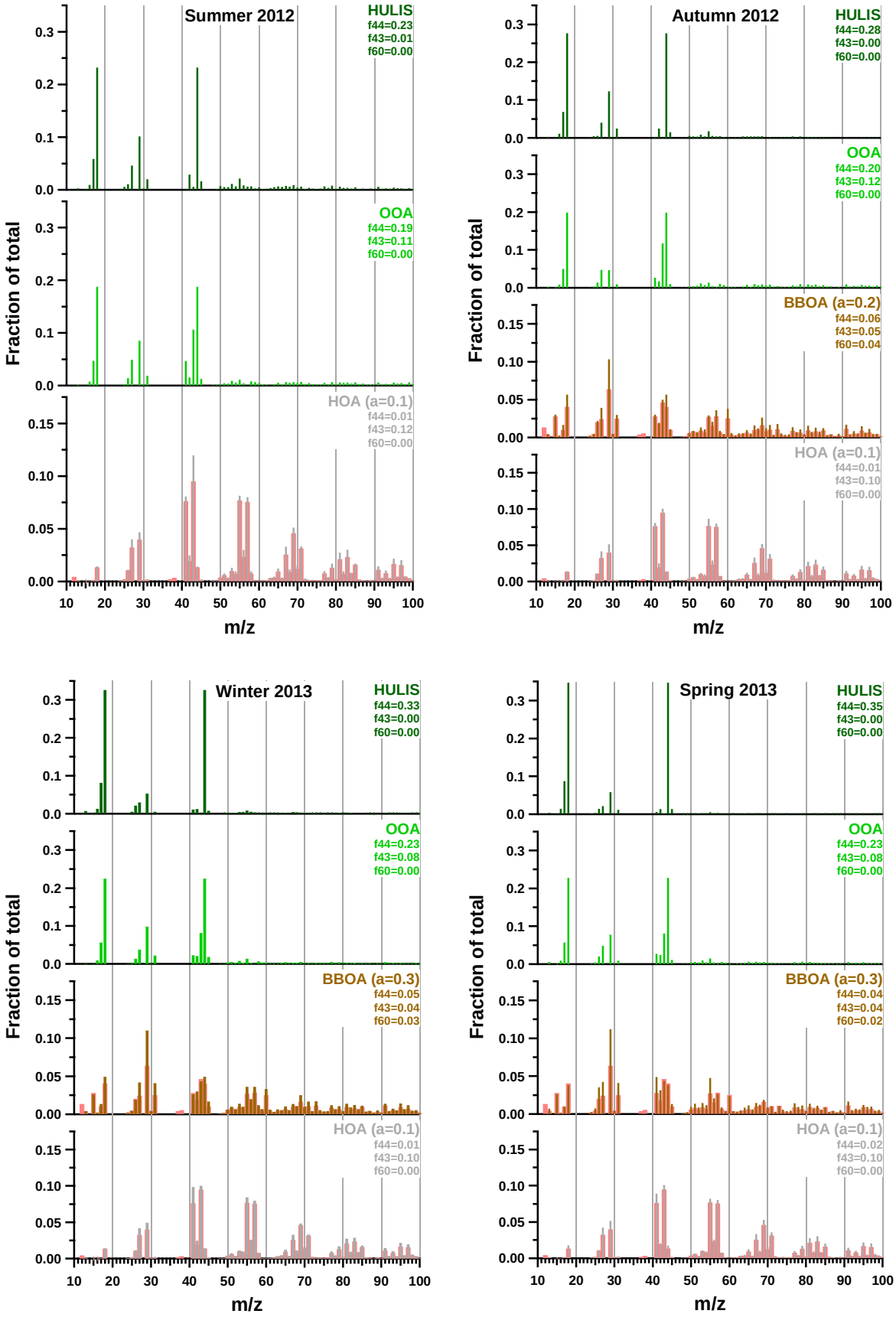

Figure S13: Mass spectra of ACSM PMF factors for each season between 2012 and 2013. For the constrained profiles HOA and BBOA, the applied a-value is written in brackets.

Corresponding reference spectra are shown by red bars. *f44*, *f43*, and *f60* are the mass fractions of m/z 44, m/z 43, and m/z 60 of the particular MS, respectively. Note that the y-axis scales of the POA are zoomed by a factor of 2 comparing to SOA profiles.

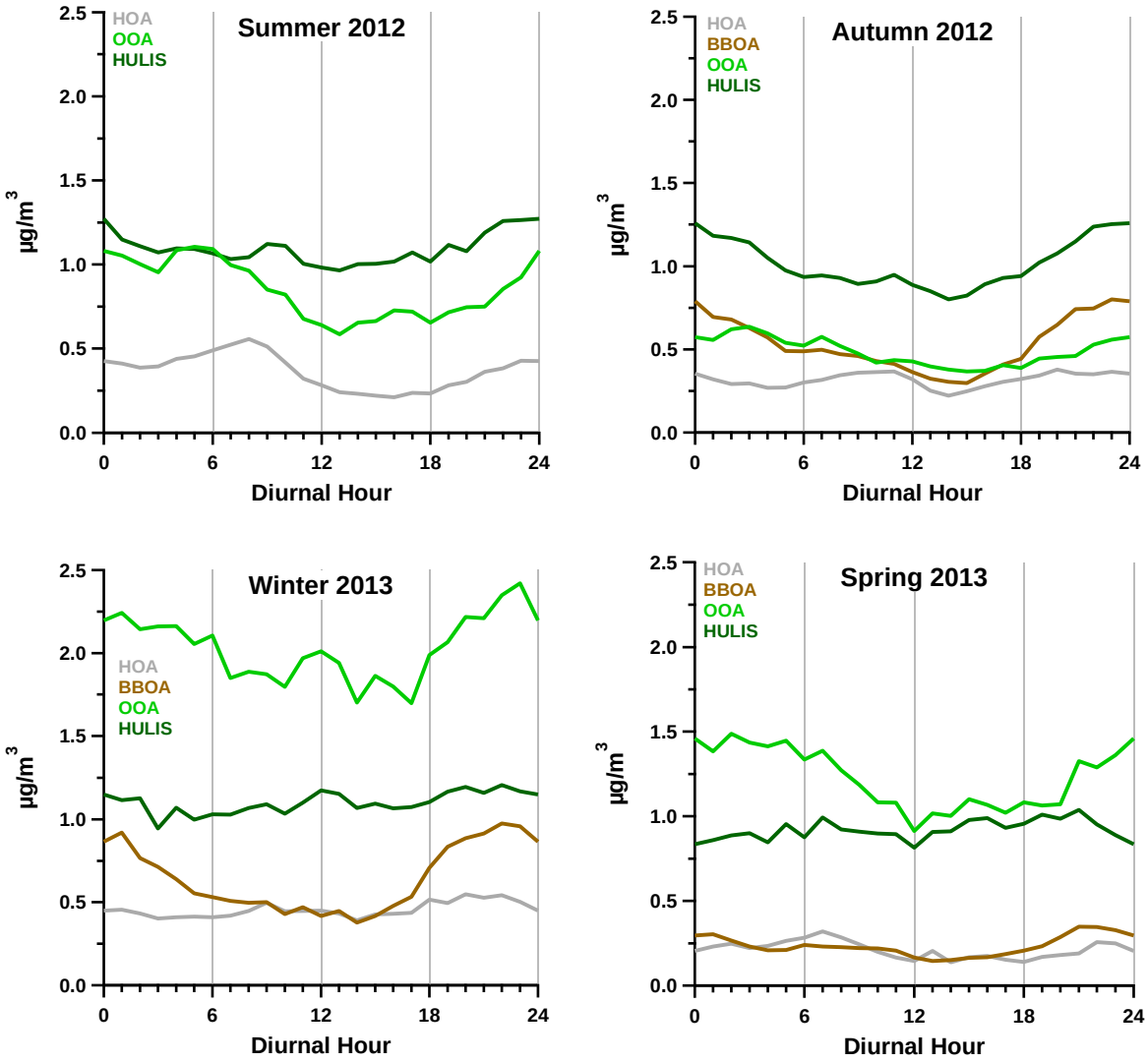

Figure S14: Average diurnal variations (local time) of ACSM PMF factors separated by season

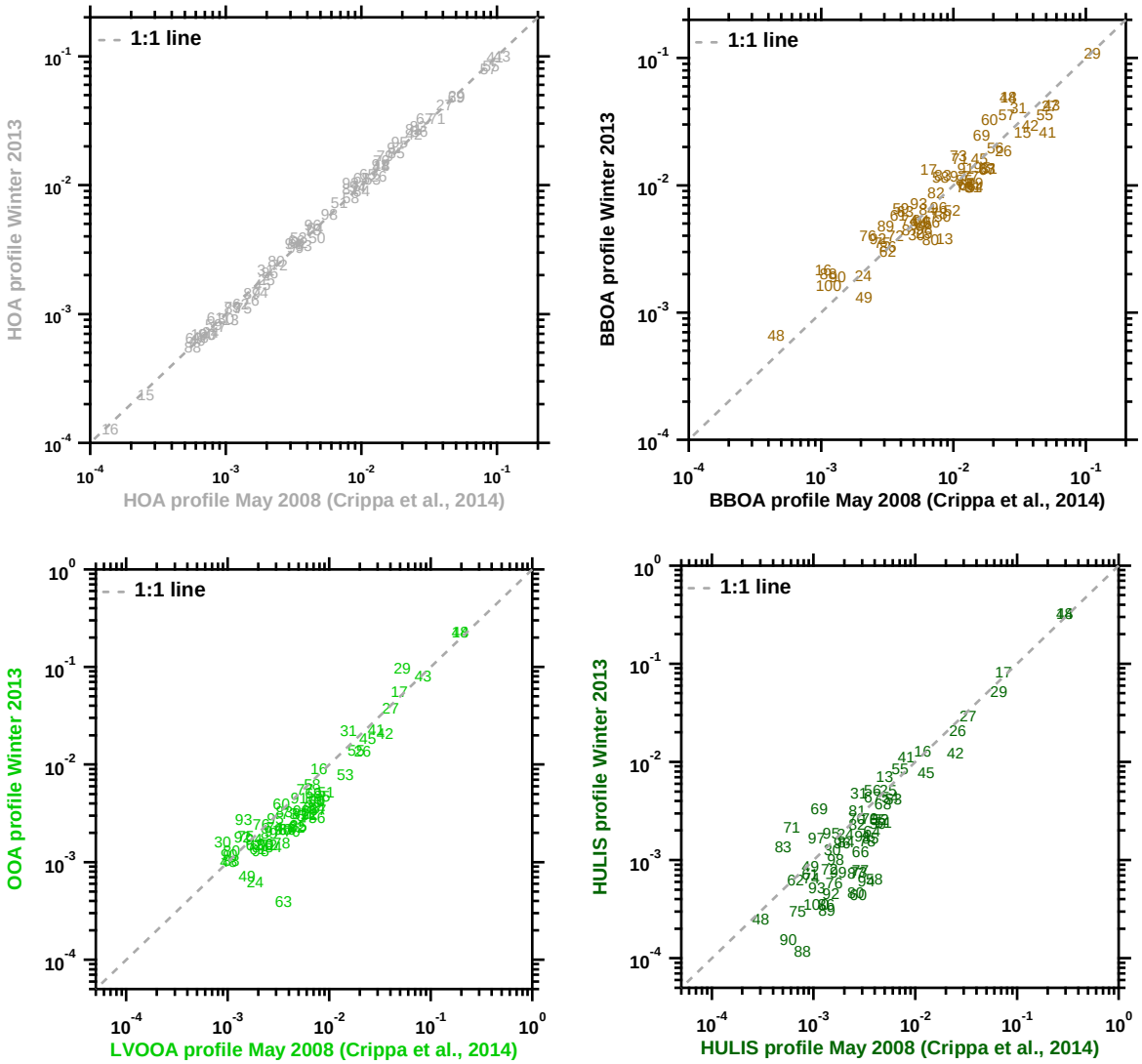

Figure S15: Scatter plots of PMF profiles from Winter 2013 vs. May 2008 as found by Crippa et al. (2014). Factor profiles from other seasons described in this work show similar correlations. The numerical markers correspond to m/z values.

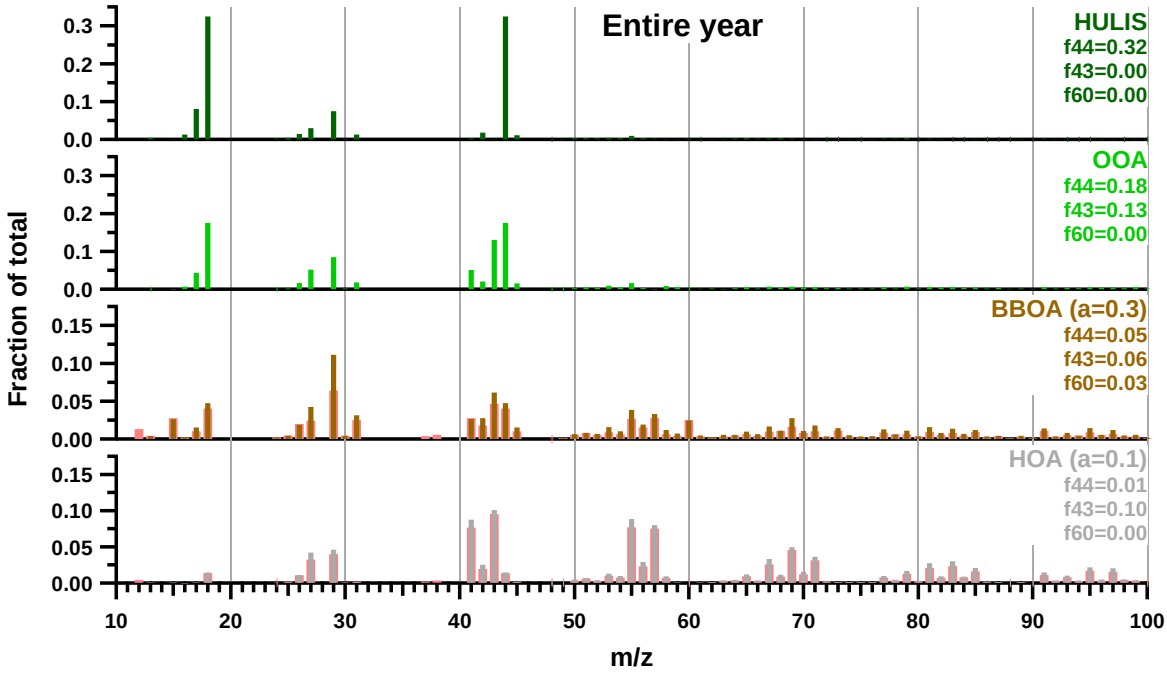

Figure S16: Mass spectra of ACSM PMF factors, derived from one single PMF exploration using the whole data set. For the constrained profiles HOA and BBOA, the applied a-value is written in brackets. Corresponding reference spectra are shown by red bars. *f44*, *f43*, and *f60* are the mass fractions of m/z 44, m/z 43, and m/z 60 of the particular MS, respectively. Note that the y-axis scales of the POA are zoomed by a factor of 2 comparing to SOA profiles.

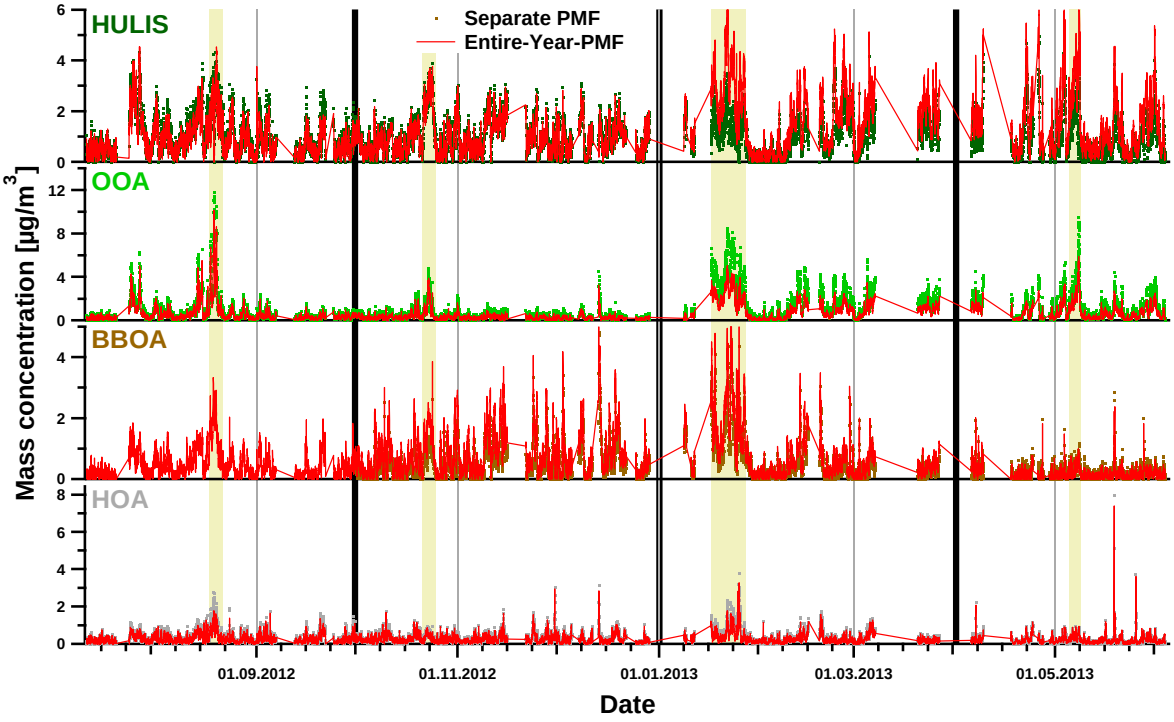

Figure S17: Time series of ACSM PMF factors. The dotted lines represent factors which are concatenated from separated solutions. Factors shown by red lines derived from one single PMF exploration using the whole data set. Pollution events are indicated by green shaded areas. Vertical lines represent the division into the four seasons.

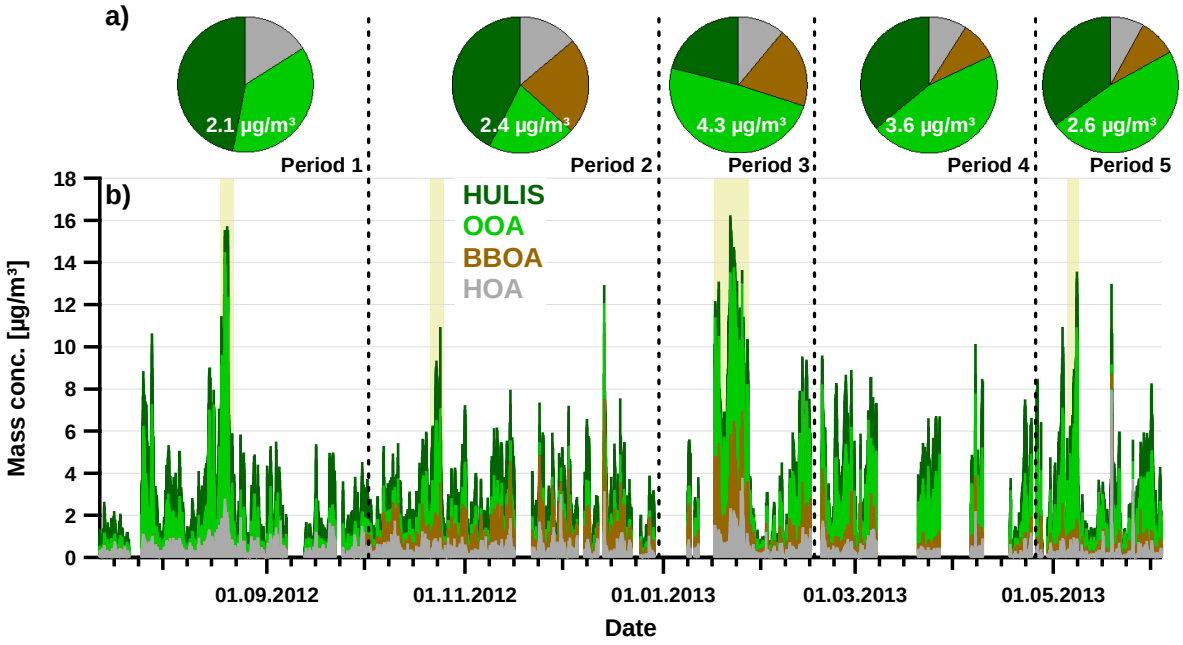

Figure S18: Overview of ACSM PMF factors: a) Pie charts of average fractional abundances of each factor, separated by the five periods as stated in Fig. 2 in the main text. The respective average total mass concentration is written inside the pie chart. b) Stacked time series of mass concentrations. Note that these plots were not obtained from one PMF exploration. Pollution events are indicated by green shaded areas.

References

Crippa, M., Canonaco, F., Lanz, V.A., Äijälä, M., Allan, J.D., Carbone, S., Capes, G., Ceburnis, D., Dall'Osto, M., Day, D.A., DeCarlo, P.F., Ehn, M., Eriksson, A., Freney, E., Hildebrandt Ruiz, L., Hillamo, R., Jimenez, J.L., Junninen, H., Kiendler-Scharr, A., Kortelainen, A.-M., Kulmala, M., Laaksonen, A., Mensah, A.A., Mohr, C., Nemitz, E., O'Dowd, C., Ovadnevaite, J., Pandis, S.N., Petäjä, T., Poulain, L., Saarikoski, S., Sellegri, K., Swietlicki, E., Tiitta, P., Worsnop, D.R., Baltensperger, U., Prevot, A.S.H., 2014. Organic aerosol components derived from 25 AMS data sets across Europe using a consistent ME-2 based source apportionment approach. Atmospheric Chemistry and Physics 14, 6159-6176.

Mensah, A.A., Holzinger, R., Otjes, R., Trimborn, A., Mentel, T.F., ten Brink, H., Henzing, B., Kiendler-Scharr, A., 2012. Aerosol chemical composition at Cabauw, The Netherlands as observed in two intensive periods in May 2008 and March 2009. Atmospheric Chemistry and Physics 12, 4723-4742.

Vermeulen, A.T., Hensen, A., Popa, M.E., van den Bulk, W.C.M., Jongejan, P.A.C., 2011. Greenhouse gas observations from Cabauw Tall Tower (1992-2010). Atmospheric Measurement Techniques 4, 617-644.